

# INVARIANT RECOGNITION OF POLYCHROMATIC IMAGES OF *Vibrio cholerae* O1

Josué Alvarez-Borrego<sup>1</sup>, Rosa Reyna Mouriño-Pérez<sup>1</sup>, Gabriel Cristóbal<sup>2</sup> and José Luis  
Pech-Pacheco<sup>1,2</sup>

<sup>1</sup>Cicese, División de Física Aplicada, Departamento de Óptica, Km. 107 Carretera Tijuana-  
Ensenada, Ensenada, B. C., México.

<sup>2</sup>Instituto de Optica (CSIC), Imaging & Vision Dept.  
Serrano 121. 28006 Madrid, Spain.

[josue@cicese.mx](mailto:josue@cicese.mx), [rmourino@cicese.mx](mailto:rmourino@cicese.mx), [gabriel@optica.csic.es](mailto:gabriel@optica.csic.es), [pech@optica.csic.es](mailto:pech@optica.csic.es)

## Abstract

Cholera is an acute intestinal infectious disease. It has claimed many lives throughout history, and it continues to be a global health threat. Cholera is considered one of the most important emergence diseases due its relation with global climate changes. The automated methods like the optical systems represent a new trend to make more accurate measurements about the presence and quantity of this microorganism in its natural environment. The automatic systems eliminate the observer bias and reduce the analysis time.

The goal of this work is evaluate the utility of coherent optical systems with invariant correlation for the recognition of *Vibrio cholerae* O1. Images of scenes were recorded with a CCD camera and decomposed in three RGB channels. A numeric simulation was developed to identify the bacteria in the different samples through an invariant correlation technique. There was not variation when we repeated the correlation and the variation between images correlation was minimum. The position, scale and rotation invariant recognition was made with scale transform through the Mellin transform. The algorithm to recognize *Vibrio cholerae* O1 was the presence of correlation peaks in green channel output and absence in red and blue channels. The discriminate criterion was the presence of correlation peaks in red, green and blue channels.

## 1. Introduction

In the eighties the estuarine origin of *Vibrio cholerae* O1 and its link with marine organisms was documented. But there are many questions about the bacteria ecology unsolved. The knowledge about its behavior in the ocean and coastal zones could led to predict the outbreaks and spread of cholera pandemics. The long-term environmental monitoring, in this case, the *Vibrio cholerae* O1 in seawater could be the answer to many of open questions around the cholera. The different human-driven techniques to recognize the bacteria have had some troubles in the reliability.

The performance of ecological studies about microscopic organisms greatly depends on the correct identification and quantification of the organism under study in natural environments. For instance, *Vibrio cholerae* O1 is responsible of cholera disease and there are many unsolved questions about its ecology that could be answered through the observation of a large number of seawater samples world-wide in order to figure it out

1-2

Microbiologists have developed several techniques for bacteria identification. *Vibrio cholerae* O1 has been usually identified through cultures in specific media and a waterfall of biochemical tests<sup>3</sup>. Nevertheless, *Vibrio cholerae* could survive in an adverse environment in a dormancy stage. This stage has been called “Viable but not culturable”, and bacteria can not be recovered by culture methods<sup>4-5</sup>. On the other hand, to develop all tests we need at least five days, and at last it is necessary to use direct methods<sup>6</sup>.

Molecular biology techniques such as Protein Chain Reaction are the most specific methods of bacteria typing. They regards the protein composition of the bacteria wall and Deoxyribonucleic acid, but they are expensive, sophisticated and complicated tools and we may not use them for screening proposal<sup>7</sup>.

Direct techniques such as stain with acridine orange and DAPI have been used too, but these are inaccurate methods that just provides information about presence of organic matter or organisms in general<sup>8-9</sup>. Direct Fluorescent Antibodies (DFA) is a fast and highly specific stain method<sup>10-12</sup>. However, the samples processed with DFA should be evaluated for an experienced observer, whose capacity depends on sample number. Slide's reading is a bored activity that consumes a lot of time, produce tiredness and decrease the observation reliability when the number of samples increases.

The different human-driven techniques to recognize bacteria have some troubles in the reliability. The automated methods like the optical systems represent a new possibility to make better measurements about the presence and quantity of this microorganism in its natural environment. Automatic systems eliminate observer bias and reduce analysis time and relieve researchers of tedious activity of organism's identification and counting and provides major effectiveness.

The use of optical systems has becoming an interesting tool for biologists, to make easier and better observations of the presence of microorganisms in an environment. Since VanderLugh introduced the filtering techniques<sup>13</sup>, optical correlation methods based on object's shape have been successfully used in pattern recognition. Several kinds of filters have been developed in order to recognise different objects. In biology, we could make

mention of the use of Circular Harmonic Filters for copepods recognition <sup>14</sup>, and matched filtering for different phytoplankton species <sup>15</sup>.

Nevertheless, bacteria recognition of particular species is a complex issue. Bacteria shape does not provide enough information to identify them, because there are many species that share the same shape. *Vibrio cholerae* O1 has a transparent curve rod shape, the same as all kind of *Vibrionaceae* family among others <sup>3</sup>. To solve this problem, we can mark *Vibrio cholerae* O1 with monoclonal antibodies and give them a specific green color<sup>12</sup> and use optical color correlation systems in order to increase the discrimination ability of pattern recognition filters, taking into account only color and shape information<sup>16-19</sup>. Bacteria color and shape depends on the illuminating wavelength, that is, color introduces additional information for improving recognition effectiveness. The logical or arithmetical sum of polychromatic object decomposition in three simple monochromatic channels (Red, Green and Blue RGB) produces a high level of recognition of targets.

Bacteria's morphology, orientation and size changes are another problems that we have to tackle. Besides shape and color, we need an optical system invariant to position, scale and rotation. We use the digital scale transform through the Mellin transform approach<sup>15</sup> in order to implement an optimal process that guarantees a high discrimination capability of invariant pattern recognition correlators. To our knowledge, this approach have never been used in color systems. Our goal is to evaluate the effectiveness of color correlation systems for *Vibrio cholerae* O1 recognition, and also develop invariant filters comparing the performance of Matched Filters with Phase-Only filters.

Section 1 presents a summary of the importance of the cholera study. Section 2 describes the invariant recognition system for cholera identification. Finally section 3 will present some results and conclusions.

## **1. Cholera Importance**

Cholera has claimed many lives throughout history, and it continues to be a global health threat. Since the first documented modern pandemic in 1817, six more pandemics have occurred<sup>20-22</sup>. The origin of these cholera pandemics is mysterious. One hypothesis holds that *Vibrio cholerae* O1 exists in a nonpathogenic state, and local environmental changes, perhaps related to the season, promote its shift to virulence<sup>4,22</sup>.

In support to this hypothesis there is a recent evidence that the cholera bacillus can survive indefinitely in some hostile natural environments.<sup>4,11,23-26</sup> The starting points for nearly all cholera epidemics appear to be port communities, implying a role for a marine transmission. We shall have to consider more carefully the possible role of the ocean in the spread of the cholera bacillus worldwide.

The biogeography of the ocean changes with the seasons, in an analogous fashion to changes on land. Most ocean cycles result from dynamic displacement of transitional, highly compressed gradients in the atmospheric and subsequent oceanic interactions.<sup>27-28</sup> Ecological studies have documented seasonal, annual, decadal, and longer-term responses to climate-driven environmental changes. Changes in species distribution and prevalence, for bacteria as well as larger organisms, also reflect climate-driven ocean variation.<sup>27-29</sup>

The long-term environmental monitoring, in this case, the *Vibrio cholerae* in seawater could be the answer to many questions around the cholera.

## 2. Invariant color object recognition

A numerical simulation was performed in order to correlate *Vibrio cholerae* O1 with Phase-only filters (POF). Figure 1 shows seven steps for invariant correlation of rotation, scale and position. All steps were developed digitally. The 1D scale transform is given by:

$$S(u_x) = \frac{1}{\sqrt{2\pi}} \int_0^{\infty} f(x) \frac{\exp(-ju_x \ln x)}{\sqrt{x}} dx \quad , \quad (1)$$

where ( $u_x$ ) is the new coordinate of the image. Because the main operation realized by lens in an optical system is the Fourier transform<sup>31</sup>, and because digitally is easier to use the fast Fourier transform (FFT), we will show that we can compute the Scale transform through the Fourier transform (whose magnitude is position invariant). This is feasible, since any linear mathematical operation, can be written in the general form

$$g(\alpha) = \int_{x_1}^{x_2} f(x) K(\alpha, x) dx \quad , \quad (2)$$

where  $g(\alpha)$  is the integration of the product of the function  $f(x)$  with the Kernel  $K(\alpha, x)$ <sup>32</sup> and  $\alpha$  is any variable. The only difference between the two transforms is thus the Kernel  $K(\alpha, x)$ .

Let's consider the Fourier transform of a function  $f(x)$ :

$$g(\alpha) = \int_{x_1}^{x_2} f(x) \exp(-j\alpha x) dx, \quad (3)$$

where  $\exp(-j\alpha x)$  is the Fourier kernel transformation. The Mellin transform can be written as:

$$g(\alpha) = \int_{x_1}^{x_2} f(x) x^{\alpha-1} dx, \quad (4)$$

where  $x^{\alpha-1}$  is the Mellin kernel transformation. Thus, it is possible to proceed from the scale to the Fourier transform via Mellin transform. In this section we will write the relation between the Scale and Mellin transform only. This is important because, of this way, equation (1) can be manipulated via Fourier transform throughout the Mellin transform easily.

The separable 2D scale transform,  $S(u_x, v_y)$  is used in this correlation process because it is invariant to size changes. Its definition is given by<sup>30</sup>:

$$S(u_x, v_y) = \frac{1}{\sqrt{2\pi}} \int_0^\infty \int_0^\infty f(x, y) \frac{\exp(-ju_x \ln x - jv_y \ln y)}{\sqrt{xy}} dx dy, \quad (5)$$



where  $(u_x, v_y)$  represent the scale variables. It is easy to show that the scale transform of the

function  $g(x, y) = \frac{f(x, y)}{\sqrt{xy}}$  is given by

$$S(u_x, v_y) = F[f(\exp(p), \exp(q))] \quad , \quad (6)$$

where F is Fourier transform.

Thus, relations between Scale with Mellin transforms in two dimensions, in one like in another sense, are<sup>33</sup>:

$$\text{Scale transform} \left[ g(x, y) = \frac{f(x, y)}{\sqrt{xy}} \right] \equiv \text{Mellin transform} [f(x, y)] \quad , \quad (7)$$

$$\text{Mellin transform} [\sqrt{xy}f(x, y)] \equiv \text{Scale transform} [f(x, y)] \quad , \quad (8)$$

So, via Mellin transform we can calculate Scale transform or viceversa. According with equation (8), between Step 2 and 3 we introduce the factor  $\sqrt{r}$  (Fig. 1), of this way, we obtain Scale transform via Mellin transform. The effect of this factor on the module of FFT is radial only.

According to Casasent and Psaltis<sup>34</sup>, it is easier to calculate an invariant correlation to scale by performing a warping of the input function and subsequently a Fourier transform (Fig.1). Initially in Step 1 (Fig.1) we have an input function  $f(x, y)$  for which a calculation of the module of the FFT  $|F(w_x, w_y)|$  (Step 2) is made; this avoids any shift of the input

function  $f(x,y)$ . When input function  $f(x,y)$  rotates, a certain angle  $\theta$ ,  $|F(w_x, w_y)|$  rotates at the same angle, and a change in scale “a” in  $f(x,y)$  magnifies  $|F(w_x, w_y)|$  by  $|a|^{-1}$ .

Effects of change in rotation and scale can be separated by polar transformation of  $|F(w_x, w_y)|$  from coordinate  $(w_x, w_y)$  to coordinate  $(r, \theta)$ . Because  $\theta = \tan^{-1}(w_y/w_x)$  and  $r = \sqrt{w_x^2 + w_y^2}$ , “a” changes the scale of  $|F(w_x, w_y)|$ , and the r-coordinate becomes  $r' = ar$  without affecting  $\theta$ -coordinate. Thus, a change in scale of bidimensional input function is a change in scale of only one dimension (r-coordinate) in the function  $F(r, \theta)$  (Step3:Fig.1). In order to keep not only the scale but the rotational invariance we will use the non-separable scale transform, by taking the log of the radial coordinate  $\mathbf{l} = \ln(\sqrt{x^2 + y^2})$

$$S(u_r, u_q) = \frac{1}{\sqrt{2\mathbf{p}}} \int_0^{\infty} \int_0^{\infty} f(\mathbf{l}, \mathbf{q}) \exp(\mathbf{l}/2) \exp(-j\mathbf{l}c_r - j\mathbf{q}c_q) d\mathbf{l} d\mathbf{q}. \quad (9)$$

Because the high frequencies present in the module of FFT have important information of features of the original images we enhance high-pass filtering effect<sup>35</sup> which consists in to apply a parabolic function to the module of FFT. In this way, low frequencies are attenuated and high frequencies are enhanced in proportion of  $w_x^2, w_y^2$ .

In Step 4 (Fig. 1), a variable change is made with respect to r:  $F(\exp(\rho), \theta)$ , where  $\rho$  is  $\ln r$ . Because in this transformation we obtain aliasing problem, we applied a bi-linear interpolation in order to avoid this effect<sup>33</sup>. In Step 5 (Fig.1) we obtain the bidimensional scale transform via a FFT. Phase-only filters  $S_{\text{POF}}(u_\rho, v_\theta)$  is defined as

$$S_{\text{POF}}(u_{\rho}, v_{\theta}) = \exp[-i\phi(u_{\rho}, v_{\theta})] \quad , \quad (10)$$

where  $|S(u_{\rho}, v_{\theta})|$  is equal to one, and  $u_{\rho}, v_{\theta}$  are variables in frequency domain (Step 6). Correlation of digital filter (Step 7) with Scale transform of the image generate a very low correlation value for geometrically dissimilar organisms and a high correlation value for geometrically similar organisms.

As it was mentioned before, the recognition of particular species of bacteria is a complex issue. Bacteria shape does not provide enough information to identify them, because there are many species that share the same shape. In specific case of *Vibrio cholerae* O1, color information is becomes an important discriminant feature, which we need to include in the whole identification process.

In general, a polychromatic object presents different shape and amplitude distribution  $A_{\lambda_i}(x,y)$  when illuminated with different wavelength  $\lambda$ . However, two different objects may present similar amplitude distribution when they are illuminated with determined wavelength  $\lambda_0$ . So, in an optical pattern recognition process using a correlator illuminated with a wavelength  $\lambda_0$ , these objects will give very similar amplitude correlation distributions, and some false alarms will appear. To avoid this problem, it is necessary to use the information about the dependence of the object amplitude distributions on wavelength<sup>36</sup>.

Most of the natural colors can be obtained as a combination of three colours (the so-called primary colors) if they are well selected. Each of them has to be on red (R), green (G), and Blue (B) regions of visible spectrum respectively. When the object is a

transparency, the amplitude transmittance obtained with illumination of one of these primaries will be called red, green and blue components of the object.

The recognition of an object in a scene is achieved by decomposing the information in three monochromatic channels and by identifying the object in each channel independently. In other words, the correlation  $C_{\lambda_i}(x,y)$  between the scene to be analyzed  $f_{\lambda_i}(x,y)$  and the bacteria to be detected  $B_{\lambda_i}(x,y)$ , in this case, are obtained by illuminating an optical set up with three wavelengths  $\lambda_i=R,G,B$  which cover the visible spectrum

$$C_{\lambda_i}(x,y) = f_{\lambda_i}(x,y) \otimes B_{\lambda_i}(x,y) \quad . \quad (11)$$

Thus, the process shown in figure 1 will be repeated for each channel (R,G, and B). In each channel, the filter to be used is matched to the corresponding component of the target. In general, objects which have a determined component  $A_{\lambda_i}(x,y)$  similar to component of the target  $B_{\lambda_i}(x,y)$  will give a maximum of correlation in this channel ( $\lambda_i$ ). But only the target will simultaneously give a correlation maximum in each channel. So, an object is detected as the target if it simultaneously produces a correlation peak in the three channels. But, in this particular case of *Vibrio cholerae* O1, we could mark it with a specific green color with monoclonal antibodies. So, the correct identification for these bacteria will be in the green channel only, and the presence of correlation peaks in the two other channels will constitute a false identification.

Therefore it is possible, with the methodology above mentioned, to recognize *Vibrio cholerae* O1 in a digital correlator invariant to rotation, position and scale changes.

### 3. Results and discussions

The recognition to scale changes was accomplished making the correlation of images of *Vibrio cholerae* 01 with differences of 20 to 150% from its original size with a delta of 5%. The 27 outcome images were correlated with a target image of original size. Both correlation coefficients results are shown in figure 2. In all cases we obtain higher correlation values though the use of the scale transform. For slightly variations from the original size the correlation value increases along both sides. We used phase-only filtering.

Correlation coefficients for 37 images of *Vibrio cholerae* 01 rotated from 0 to 360° with and without scale transform are shown (Fig. 3). The invariant correlation coefficients were higher. In the output, there is a change in the position of the correlation peak regarding the sizes and angles differences with the filter organism.

Some examples of invariant correlation outputs in green channel of *Vibrio cholerae* 01, using the methodology shown in figure 1, are shown (Figs. 4-5). Figure 4e shows an image with three bacterias with the same angle but for three different sizes (120%, 100% and 60%) respect to the filter (Fig. 4f). The output in the green channel shows three peaks to 0° degrees (Fig. 4a). A profile of these peaks are shown in figure 4c. The one in the middle corresponds to the 100% and the one besides the left to the 60% and the one besides the right to the 120%. Another peaks at 180° are present because the periodicity produced by the polar transform.

Invariant correlation results in green channel with a filter that has an organisms of different size and orientation ( $90^\circ$ ) (Fig. 4h) are shown (Fig. 4b). Three correlation peaks are present at  $90^\circ$  that is the angle of bacteria in image (Fig. 4g) with respect to bacteria in the filter. A profile of the lines 55, 60 and 65 shows three correlation peaks (Fig. 4d). The left arrow represents larger bacteria, the arrow in the center the middle organisms and the right arrow the smallest.

Figures 5e and 5g present two organisms with minimal scale and rotation differences. This image was correlated with a filter with the same orientation and similar size (Fig. 5f). We observe a unique correlation peak at  $0^\circ$  and its harmonic at  $180^\circ$  (Fig. 5a). A profile of this result is shown in figure 5c. Even there are two bacteria in the image test, there is just one peak in the output because when the organisms are similar in size and orientation the peaks are superimposed. This constitutes a tradeoff for organisms count, but this invariant process improves the the recognition efficiency because the correlation is invariant to position, scale and rotation.

We can see similar results in figures 5b and 5d also in the green channel. The filter image (Fig. 5h) is a bacteria different in rotation and a little in scale. The peak is now in  $90^\circ$  because the bacteria is  $90^\circ$  in orientation with respect to the image test.

These results show that it is possible to recognize the bacteria *Vibrio cholerae* 01 in the green channel irrespective to to size, orientation and position changes. Only bacterias *Vibrio cholerae* 01 can be recognized in the green channel. The presence of correlation peaks in the other two channels is a false identification.

#### 4. References

1. R.R. Colwell. "Global climate and infectious disease: The cholera paradigm,". *Science*, **274**:2025-2031, (1996)
2. R.R. Mouriño-Pérez "Oceanography and the seventh cholera pandemic" *Epidemiology*, **9**(3):355-357, (1998)
3. K. Wachsmuth, G.K. Morris, J. C. Feeley. "Vibrio," In: E. H. Kennette, A. Balows, W. J. Hausler, J. P. Truant. *Manual of Clinical Microbiology*. 3<sup>rd</sup> ed. (American Society for Microbiology, Washington, D.C., 1980) pp 226-234
4. R. R. Colwell, A. Huq. "Vibrios in the environment: viable but nonculturable *Vibrio cholerae*" .In: *Vibrio cholerae* and Cholera: Molecular to Global Perspectives. (American Society for Microbiology, Washington DC, 1994), pp.117-134.
5. H-S Xu, N. Roberts, L. Singleton, R. W. Attwell, D. J. Grimes, R. R. Colwell "Survival and Viability of Nonculturable *Escherichia coli* and *Vibrio cholerae* in the estuarine and marine environment," *Microb. Ecol.*, **8**:313-323, (1982)
6. Manual Food and Drug Administration. 1992. *Bacteriological Analytical Manual*. 7th ed. AOAC International, Arlington, Virginia, 529 pp. ????
7. P.I. Fields, T. Popovic, K. Wachsmuth, O. Olsvik. "Use of polymerase chain reaction for detection of toxigenic *Vibrio cholerae* O1 strains from the Latin american cholera epidemic," *J. Clin. Microbiol.*; **30**(8):2118-2121, (1992)
8. M. T. Suzaki, E. B. Shen, B. F. Sherr. "DAPI direct counting underestimates bacterial abundances and average cell size compared to AO direct counting,". *Limnol. Oceanogr.* **38**(7):1566-1570, (1993)

9. Back J. P., R.G. Kroll, 1991. The differential fluorescence of bacteria stained with acridine orange and the effects of heat. *J. Appl Bacteriol*, 71:51-58
10. P. R. Brayton, R. R. Colwell. "Fluorescent antibody staining method for enumeration of viable environmental *Vibrio cholerae* O1,". *J. Microbiol. Methods*. **6**:309-314, (1987)
11. Huq, R. R. Colwell, R. Rahman, A. Ali, A. R. Chowdhury, S. Parveen, D.A. Sack, E. Russek-Cohen. "Detection of *Vibrio cholerae* O1 in the aquatic environment by fluorescent-monoclonal antibody and culture methods," *Appl. Environm. Microbiol.* **56**(8):2370-2373 (1990)
12. J. A. K. Hasan, D. Bernstein, A. Huq., L. Loomis., M. L. Tamplin, R. R. Colwell. "Cholera DFA: An improved direct fluorescent monoclonal antibody staining kit for rapid detection and enumeration of *Vibrio cholerae* O1," *FEMS Microbiol Letters*. **120**:143-148 (1994)
13. VanderLugt, "Signal detection by complex spatial filter" *IEEE Trans. Inf. Theory* **IT-10**, 139-145 (1964)
14. V. A. Zavala-Hamz, J. Alvarez-Borrego. "Circular harmonic filters for the recognition of marine microorganisms" *Appl. Opt.* **36**:484-489 (1997)
15. J. L. Pech-Pacheco, J. Alvarez-Borrego. "Optical-digital system applied to the identification of five phytoplankton species" *Marine Biology*. **132**, 357-365 (1998)
16. M. S. Millán, J. Campos, C. Ferreira, M. J. Yzuel. "Matched filter and phase only filter performance in colour image recognition,". *Optics Communications*. **73**(4), 277-284 (1989)
17. M. S. Millán, M. J. Yzuel, J. Campos, C. Ferreira. "Strategies for the color character recognition by optical multichannel correlation,". *SPIE*. **1507**, 183-197 (1991)



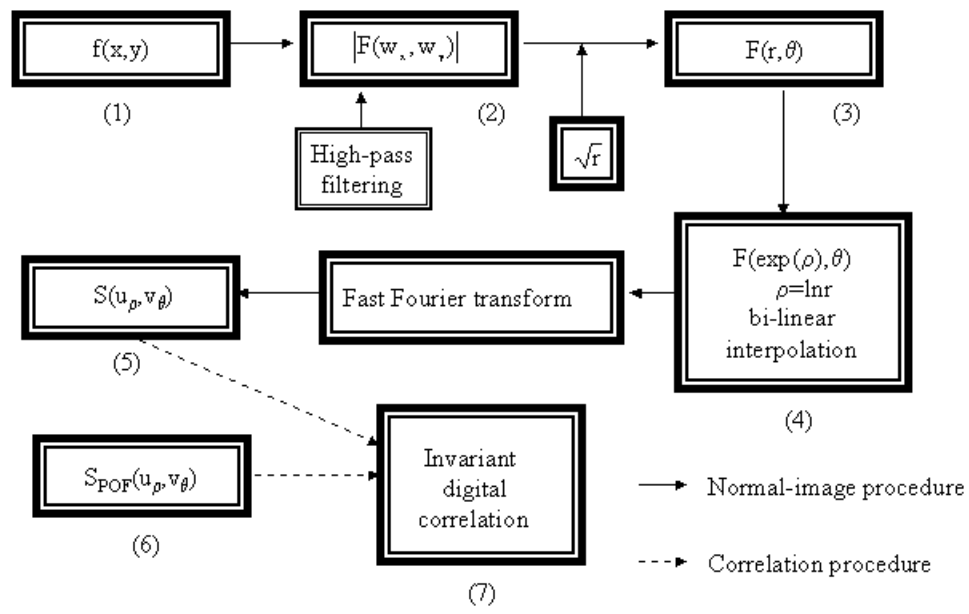
18. M.S. Millán, N. Vila, M. J. Yzuel. "Colour reversal films in multichannel optical correlators for polychromatic image recognition,". *Pure Appl. Opt.* **1**, 199-218 (1992)
19. V. Kober, V. Lashn, I. Moreno, J. Campos. "Color component transformations for optical pattern recognition," *J. Opt. Soc. Am.* **14**, 2656-2669 (1997)
20. P. Blake. "Historical perspectives on pandemic cholera," In: *Vibrio cholerae* and Cholera: Molecular to Global Perspectives. (American Society for Microbiology Washington D.C., 1994), pp.293-295.
21. J. Fernández-de Castro. "El cólera: un problema no resuelto," *Ciencias.* **24**, 33-44. (1991)
22. R. Tauxe, L. Seminario, R. Tapia, M. Libel. "The Latin American epidemic,". In: *Vibrio cholerae* and Cholera: Molecular to Global Perspectives. (American Society for Microbiology Washington D.C., 1994), pp.321-345.
23. F. L. Singleton, R. Attwell, M. S. Jangi, R. R. Colwell. "Effects of temperature and salinity on *Vibrio cholerae* growth," *Appl. Environ. Microbiol.* **44**, 1047-1058 (1982)
24. F. L. Singleton, R. Attwell, M. S. Jangi, R. R. Colwell. "Influence of salinity and organic nutrients concentration on survival and growth of *Vibrio cholerae* in aquatic microcosms," *Appl. Environ. Microbiol.* **43**, 1080-1085 (1982)
25. M. L. Tamplin, R. R. Colwell. "Effects of microcosm salinity and organic substrate concentration on production of *Vibrio cholera* enterotoxin," *Appl. Environ. Microbiol.* **52**, 297-301 (1982)
26. J. Byrd, H-S Xu, R. R. Colwell. "Viable but nonculturable bacteria in drinking water,". *Appl. Environ. Microbiol.* **57**, 875-878 (1991)

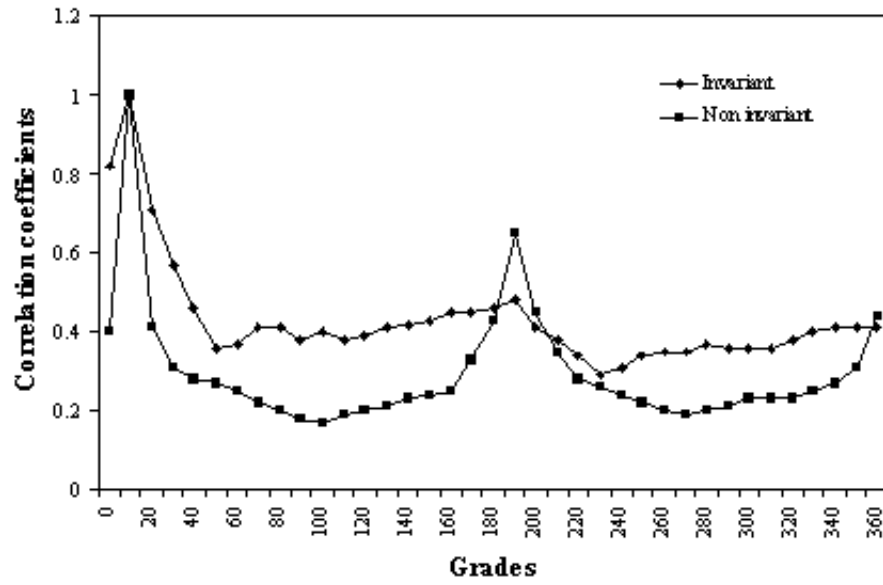
27. D. Sharp, D. R. McLain. "Comments on the global ocean observing capabilities, indicator species as climate proxies, and the need for timely ocean monitoring,". *Oceanography*. **5**, 163-168 (1992)
28. K. H. Mann, J. R. N. Lazier. "Dynamics of marine ecosystems: biological-physical interactions in the oceans," (Blackwell Science, Cambridge, MA, 1991) pp.459
29. P. R. Epstein. "Emerging diseases and ecosystems instability: new threats to public health," *Am. J. Public Health*. **85**, 168-172 (1995)
30. L. Cohen, "Time-frequency analysis", Prentice Hall Signal Processing Series, Upper Saddle River, New Jersey 07458, (1995).
31. J. Goodman, "Introduction to Fourier optics. McGraw-Hill, New York, 1968.
32. Arfken G, "Mathematical methods for physicists. 3<sup>rd</sup> edn. Academic Press, Inc. Harcourt Brace Jovanovich, San Diego, (1981).
33. J. A. Cuesta Merino, "Aplicación de la transformada de escala en el análisis de imágenes", Universidad Politécnica de Madrid, Escuela Técnica Superior de Ingenieros en Telecomunicación, Proyecto de fin de carrera, (1999).
34. Casasent D. and Psaltis D, "Scale invariant optical transform". *Optical Engineering*, **15**(3), 258-261, (1976).
35. Pech-Pacheco J. L., Cristóbal, G. , Alvarez-Borrego, J. and Keil, M., Automatic object identification irrespective to geometric changes. Submitted to *Applied Optics*
35. J. Campos, M. S. Millan, M. J. Yzuel, C. Ferreira, "Colour invariant character recognition and character-background colour identification by multichannel matched filter", *SPIE*, Vol. 1564, pp.189-198, (1991).

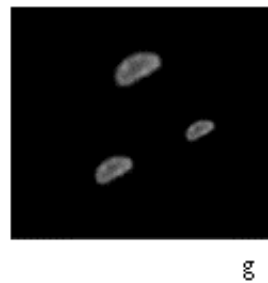
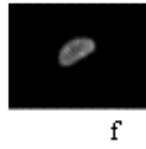
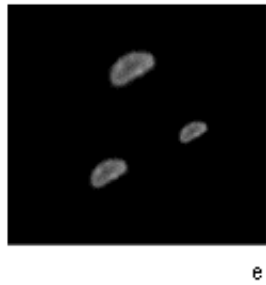
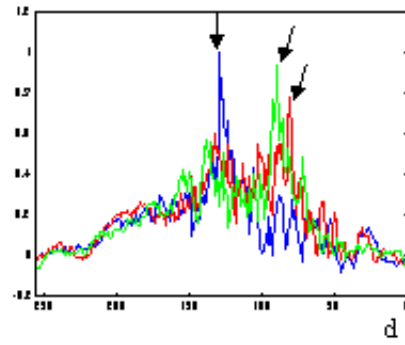
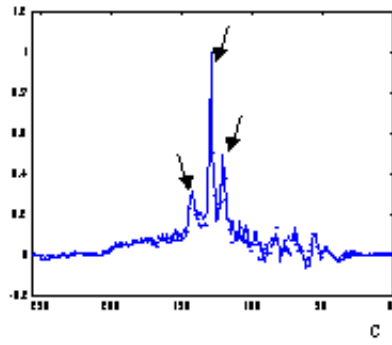
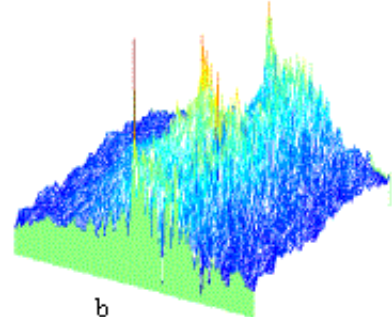
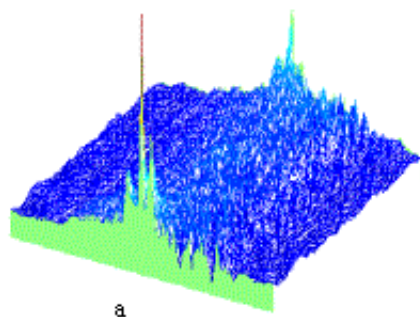
36. Cristobal, G. and Cohen, L. "Scale in images", Proc. SPIE, Advanced Signal Processing. Algorithms, Architectures and Implementations VI, Vol. 2846, pp. 251-261, (1996).

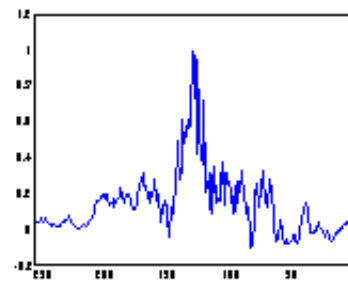
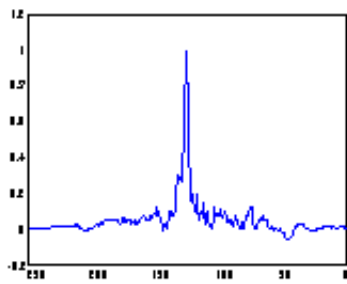
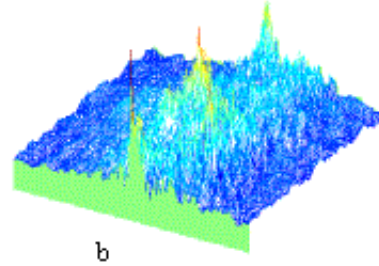
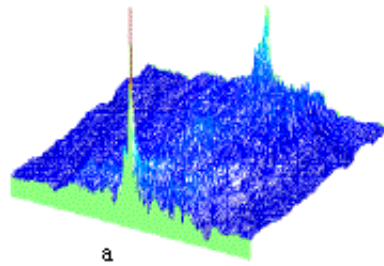
**Figures captions**

- Figure 1 Steps of scale transform via Mellin transform
- Figure 2 Correlation coefficients of scaled images from 20 to 150% with a delta of 5%.
- Figure 3 Correlation coefficients of rotated images from 0 to 360° with a delta of 10°.
- Figure 4 Correlation with scale transform via Mellin transform. a) and b) Correlation output in green channel with phase only filters, c) Graph of lines 1 and 2 of clause (a), d) Graph of lines 55, 60 and 65 of clause (b), e) and g) Problem images in green channel, and f) and h) Filter image in green channel.
- Figure 5 Correlation with scale transform via Mellin transform. a) and b) Correlation output in green channel with phase only filters, c) Graph of line at 0° of clause (a), d) Graph of line at 90° of clause (b), e) and g) Problem images in green channel, and f) and h) Filter image in green channel.









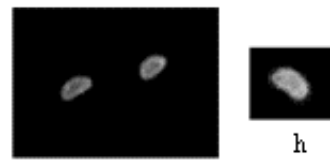
c

d



f

e



h

g